Vietnam Journal of Science and Technology ***61*** *(3) (2023) 506-518*

doi:10.15625/2525-2518/17666

Free vibration of axially loaded microbeam in MEMS based on sinusoidal shear deformation theory

Cong Ich Le[1, *], Dinh Kien Nguyen[2, 3]

[1]*Department of Machinery Design, Le Quy Don Technical University, 236 Hoang Quoc Viet, Bac Tu Liem, Ha Noi, Viet Nam*

[2]*Department of Solid Mechanics, Institut of Mechanics, Vietnam Academy of Science and Technology, 18 Hoang Quoc Viet, Cau Giay, Ha Noi, Viet Nam*

[3]*Graduate University of Science and Technology, Vietnam Academy of Science and Technology, 18 Hoang Quoc Viet, Cau Giay, Ha Noi, Viet Nam*

[*]Email: *lecongich79@lqdtu.edu.vn*

Received: 28 February 2022; Accepted for publication: 14 January 2023

Abstract. Free vibration of a silicon microbeam in micro-electromechanical systems (MEMS) subjected to electrostatic and axial forces is studied in the framework of a sinusoidal shear deformation theory. A nonlinear finite element formulation based on the von Kármán nonlinear assumption and the modified couple stress theory (MCST) is formulated and employed to establish the discrete nonlinear governing equations for the microbeam. The deflection of the microbeam at a given direct current (DC) voltage is firstly calculated by the Newton Raphson method and used to evaluate the natural frequencies. The influence of the applied voltage and the microsize effect on the frequencies is investigated in detail. The results reveal that the microstructural parameter has an important role in the vibration the microbeam, and the natural frequencies are underestimated by ignoring the microstructural parameter. The dependence of the pull-in voltage upon the material length microscale and the axial force is also examined and discussed.

Keywords: Microbeam, Sinusoidal theory, MCST, MEMS, Vibration.

Classification numbers: 5.2.1, 5.2.4, 5.4.2.

1. INTRODUCTION

Microbeams are found in many micro-electromechanical system (MEMS) devices, e.g. capacitive MEMS switches and resonators, filters, and resonant sensors. Accurate prediction of frequencies of the microbeams is crucial for correct use of the microbeams. Due to the electric actuation, deflections of the microbeams in MEMS are usually large, and thus nonlinear analyses are necessary to adopt in predicting mechanical characteristics of the MEMS microbeams. Various methods have been developed for assessing the mechanical behaviour of microbeams actuated by electric and mechanical forces.

In the early works, the small size effect has not been taken into consideration in analysing MEMS microbeams. For example, Choi and Lovell [1] adopted the traditional Euler-Bernoulli beam theory to compute deflections and stresses of clamped microbeams subjected to both the electrostatic and mechanical forces. Abdel-Rahmanet *et al.* [2] proposed a nonlinear model of microbeams accounting for electrostatic forcing and restoring force for estimation of deflections and frequencies of MEMS microbeams. The static and dynamic pull-in behaviour of an axially loaded MEMS microbeam due to the electric actuation was investigated by Younis *et al.* [3], taking into account the viscous damping effect. Younis and Nayfeh [4] derived the first-order nonlinear differential equations for analyzing a resonant microbeam subjected to an electric actuation and an axial force. The response of a microbeam-based resonant sensor to super-harmonic and sub-harmonic electric actuations was investigated in [5] using the perturbation method. The pull-in phenomenon of electrostatically actuated microcantilever beams actuated by electrostatic force was considered by Chaterjee and Pohit [6]. Finite element method was adopted by several authors to study the pull-in phenomenon of MEMS microbeams [7, 8]. In these works, the deformation of the microbeams was modelled by using the traditional Euler-Bernoulli beam theory. A commercial finite element software named COMSOL was employed by Kaneria *et al.* [9] in their study of the pull-in phenomenon of microcantilever in MEMS devices.

The influence of the microsize effect on the behaviour of MEMS microbeams was recently considered. The modified couple stress theory (MCST) was used in combination with Euler-Bernoulli beam theory by Farokhi and Ghayesh [10] to construct the equation of motion for computing dynamic response of a MEMS microcantilever under an electric excitation. It has been shown by the authors that an overestimated deflection is obtained, while the static pull-in voltage is underestimated when the microsize effect is not taken into account. Ghayesh and Farokhi [11] modelled the electrode in MEMS by a microplate to study the nonlinear behaviour of MEMS resonators actuated by electric force. The static pull-in phenomenon of microcantilevers in MEMS, taking the microsize effect into account, was studied by Baghani [12] using an analytical method. The method based on the modified variational iteration procedure allows to evaluate the nonlinear response of the microbeams to electric actuation. The size-dependent resonant phenomenon of MEMS resonators simultaneously subjected to DC and AC voltages was considered by Ghayesh *et al.* [13] within the framework of Euler-Bernoulli beam theory and the MCST. The Galerkin method was adopted by the authors to compute the frequency-response curves.

In this paper, the free vibration of a clamped silicon microbeam in MEMS with an axial force is investigated by finite element method. The microsize effect is modelled via the MCST, and the deformation of the microbeam is described by sinusoidal shear deformation theory. As mentioned above, defections of the microbeam under the electric force in MEMS are relatively large, and they should be computed before evaluating the frequencies. To this end, the von Kámán nonlinear strain-displacement assumption is employed herein to derive a two-node beam element, the Newton-Raphson method is firstly used to compute the beam deflections. With the obtained deflection, the tangent stiffness matrix is evaluated, and then used to construct the eigenvalue problem. The natural frequencies are computed for the microbeam under different voltages and axial forces. The influence of the microsize effect, the applied voltage and the axial force on the frequencies of the microbeam is studied in detail and highlighted. The dependence of the pull-in voltage at which the instability occurs is also examined and discussed.

2. MATHEMATICAL FORMULATION

Figure 1 shows a clamped microbeam with length L, rectangular cross section formed one side of a capacitor [4, 13]. Shown in the figure, h, b and d, respectively, are the height, width of the beam, and the air-gap between the electrode and the microbeam. The x-axis of the Cartesian system (x, z) in Figure 1 is chosen on the mid-plane, and the z-axis directs upwards.

In order to account for the microstructural effect, the MCST with only one microscale parameter proposed by Yang *et al.* [14] is employed in the present work to calculate the strain energy of the microbeam as follows

$$U_b = \frac{1}{2}\int_V (\boldsymbol{\sigma} : \boldsymbol{\varepsilon} + \mathbf{m} : \boldsymbol{\chi}) \mathrm{d}V \tag{1}$$

In the above equation, V is the volume of the microbeam; σ and ε denote the stress and strain tensors, respectively; m is the deviatoric part of the couple stress tensor, and χ is the symmetric curvature tensor.

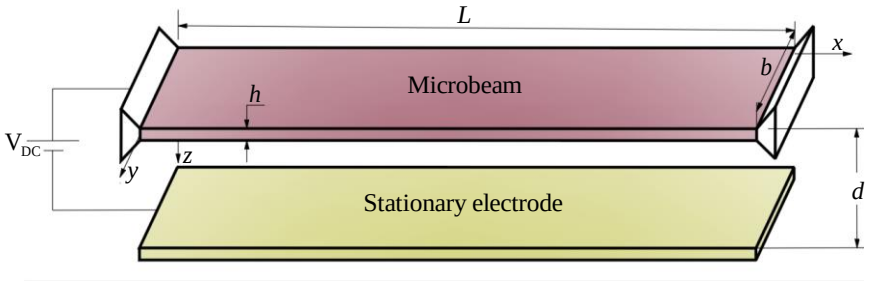

Figure 1. Model of a clamped microbeam in MEMS

The components of the symmetric curvature tensor are defined as

$$\chi_{ij} = \frac{1}{2}\left(\frac{\partial \theta_i}{\partial x_j} + \frac{\partial \theta_j}{\partial x_i}\right), \; i, j = 1, 2, 3 \tag{2}$$

where θ_i (i = 1, 2, 3) are the components of the rotation vector that can be expressed as

$$\boldsymbol{\theta} = [\theta_1, \; \theta_2, \; \theta_3] = \frac{1}{2}\begin{vmatrix} \vec{i} & \vec{j} & \vec{k} \\ \partial/\partial x & \partial/\partial y & \partial/\partial z \\ u_1 & u_2 & u_3 \end{vmatrix} \tag{3}$$

where u_1, u_2 and u_3 are the displacements in the x, y and z directions, respectively.

The components of the deviatoric part of the couple stress tensor based on the linear behaviour of the beam material can be written as

$$m_{ij} = 2Gl^2 \chi_{ij} \tag{4}$$

where $G = \dfrac{E}{2(1+\nu)}$ is the shear modulus, l is the material length microscale parameter; E and ν are Young's modulus and Poisson's ratio, respectively.

According to the sinusoidal shear deformation theory [15], the displacements u_1, u_2 and u_3, are respectively given by

$$u_1 = u_0(x,t) - zw_{b,x}(x,t) - \left[z - \frac{h}{\pi}\sin\left(\frac{\pi z}{h}\right) \right] w_{s,x}(x,t)$$
$$u_2 = 0, \qquad u_3 = w_b(x,t) + w_s(x,t) \tag{5}$$

where $u_0(x,t)$, $w_b(x,t)$ and $w_s(x,t)$ denote the in-plane displacement in x-direction, the bending and shear components of the transverse displacement, respectively. In equation 5 and hereafter, the subscript comma denotes the derivative with respect to the spatial variable x, e.g. $w_{b,x} = \partial w_b / \partial x$.

Based on the von Kármán nonlinear assumption, the normal and shear strains deduced from equation 5 are as follows

$$\varepsilon_x = u_{0,x} + \frac{1}{2}(w_{b,x} + w_{s,x})^2 - zw_{b,xx} - f(z)w_{s,xx},$$
$$\gamma_{xz} = g(z)w_{s,x} \tag{6}$$

with

$$f(z) = z - \frac{h}{\pi}\sin\frac{\pi z}{h},$$
$$g(z) = 1 - f_{,z}(z) \tag{7}$$

Based on the Hook's law, the constitutive equations of the beam material are

$$\sigma_{xx} = E\varepsilon_{xx},$$
$$\tau_{xz} = G\gamma_{xz} \tag{8}$$

In this case, the tensors in equation 1 can be expressed as

$$\boldsymbol{\sigma} = \begin{bmatrix} \sigma_{xx} & 0 & \tau_{xz} \\ 0 & 0 & 0 \\ \tau_{xz} & 0 & 0 \end{bmatrix}, \ \boldsymbol{\varepsilon} = \begin{bmatrix} \varepsilon_{xx} & 0 & \frac{\gamma_{xz}}{2} \\ 0 & 0 & 0 \\ \frac{\gamma_{xz}}{2} & 0 & 0 \end{bmatrix}, \ \boldsymbol{\chi} = \begin{bmatrix} 0 & \chi_{xy} & 0 \\ \chi_{xy} & 0 & 0 \\ 0 & 0 & 0 \end{bmatrix}, \ \mathbf{m} = 2Gl^2\boldsymbol{\chi} \tag{9}$$

with

$$\chi_{xy} = -\frac{w_{b,xx} + w_{s,xx}}{2} + g_{,z}\frac{w_{s,xx}}{4} \tag{10}$$

Using equation 9, one can recast the strain energy in equation 1 in the form

$$U_b = \frac{b}{2}\int_0^L \int_{-h/2}^{h/2} \left(\sigma_{xx}\varepsilon_{xx} + \tau_{xz}\gamma_{xz} + 2m_{xy}\chi_{xy}\right) \mathrm{d}z\mathrm{d}x$$
$$= \int_0^L \left\{ \frac{EA}{8}\left(2u_{0,x} + w_{b,x}^2 + 2w_{b,x}w_{s,x} + w_{s,x}^2\right)^2 + EI\left(\frac{w_{b,xx}^2}{2} + w_{s,xx}^2\left(\frac{1}{2} + \frac{3}{\pi^2} - \frac{24}{\pi^3}\right) \right.\right.$$
$$\left.\left. + w_{b,xx}w_{s,xx}\left(1 - \frac{24}{\pi^3}\right)\right) + GA\frac{w_{s,x}^2}{4} + GAl^2\left(\frac{w_{b,xx}^2}{2} + \frac{w_{s,xx}^2}{2}\left(\frac{9}{16} - \frac{1}{\pi}\right)\right)\right\} \mathrm{d}x \tag{11}$$

The kinetic energy of the microbeam deduced from equation 1 is as follows

$$T_b = \frac{1}{2}\int_V \rho\left(\dot{u}_1^2 + \dot{u}_3^2\right)\mathrm{d}V = \frac{\rho b}{2}\int_0^L \int_{-h/2}^{h/2} \left[\left(\dot{u}_0 - z\dot{w}_{b,x} - f(z)\dot{w}_{s,x}\right)^2 + \left(\dot{w}_b + \dot{w}_s\right)^2 \right] \mathrm{d}z\mathrm{d}x$$

$$= \int_0^L \left\{ \rho A \left[\frac{\dot{u}_0^2}{2} + \frac{\dot{w}_b^2}{2} + \frac{\dot{w}_s^2}{2} + \dot{w}_b \dot{w}_s \right] + \rho I \left[\frac{\dot{w}_{b,x}^2}{2} + \dot{w}_{s,x}^2 \left(\frac{1}{2} + \frac{3}{\pi^2} - \frac{24}{\pi^3} \right) + \dot{w}_{b,x} \dot{w}_{s,x} \left(1 - \frac{24}{\pi^3} \right) \right] \right\} \mathrm{d}x \tag{12}$$

where ρ is the mass density. The over dot in equation 12 and hereafter denotes the derivative with respect to the time variable t (the corresponding velocity).

The beam subjected to the electrostatic force per unit length has the form [10, 13]

$$q(x,t) = \frac{\varepsilon_0 b \mathrm{V}_{\mathrm{DC}}^{\ 2}}{2\left(d - u_3(x,t)\right)^2} \tag{13}$$

where V_{DC} is the DC polarization voltage, and ε_0 is the dielectric constant of vacuum.

The work done by the electric force is given by [10]

$$W_F = \int_0^L q(x,t) u_3 \mathrm{d}x \tag{14}$$

The microbeam is also considered to be subjected to an axial force P, resulting in the energy W_P of the form

$$W_P = \frac{1}{2} \int_0^L P u_{3,x}^2 \mathrm{d}x = \frac{1}{2} \int_0^L P \left(w_{b,x} + w_{s,x} \right)^2 \mathrm{d}x = \frac{1}{2} \int_0^L P \left(w_{b,x}^2 + w_{s,x}^2 + 2 w_{b,x} w_{s,x} \right) \mathrm{d}x \tag{15}$$

Applying Hamilton's principle to energy expressions given by equations 11, 12, 14, and 15 leads to nonlinear differential equations of motion for the microbeam. However, it is difficult to derive a closed-form solution for such equations, and a finite element formulation is derived in the next section to establish the discretized equation of motion for the microbeam.

3. FINITE ELEMENT FORMULATION

The discretized equation of motion is established in this section by using a finite element formulation. To this end, we consider herewith a two-node beam element with length l_e. The vector of nodal displacements (d_e) with ten degrees of freedom has the form

$$\underset{10\times1}{\mathbf{d}_e} = \left\{ \mathbf{u}^e \ \ \mathbf{w}_b^e \ \ \mathbf{w}_s^e \right\}^T \tag{16}$$

where

$$\mathbf{u}^e = \left\{ u_{01} \ u_{02} \right\}^T, \quad \mathbf{w}_b^e = \left\{ w_{b1} \ w_{b,x1} \ w_{b2} \ \ w_{b,x2} \right\}^T, \quad \mathbf{w}_s^e = \left\{ w_{s1} \ w_{s1,x} \ w_{s2} \ \ w_{s2,x} \right\}^T \tag{17}$$

are the element vectors of nodal axial displacements, bending and shear parts of the transverse displacements, respectively.

The displacements inside the element are interpolated according to

$$u_0 = \mathbf{N}\mathbf{u}^e, \quad w_b = \mathbf{H}\mathbf{w}_b^e, \quad w_s = \mathbf{H}\mathbf{w}_s^e \tag{18}$$

where $\mathbf{N} = \left\{ N_1 \ N_2 \right\}$ and $\mathbf{H} = \left\{ H_1 \ H_2 \ H_3 \ H_4 \right\}$ are the matrices of the shape functions. The following linear and Hermite shape functions are employed here with

$$N_1 = 1 - \frac{x}{l},\ N_2 = \frac{x}{l}$$
$$H_1 = 1 - 3\frac{x^2}{l^2} + 2\frac{x^3}{l^3},\ H_2 = x - 2\frac{x^2}{l} + \frac{x^3}{l^2},\ H_3 = 3\frac{x^2}{l^2} - 2\frac{x^3}{l^3},\quad H_4 = -\frac{x^2}{l} + \frac{x^3}{l^2} \tag{19}$$

With the interpolations, one can express the strain energy in equation 11 in the following form

$$\begin{aligned} U_b = \frac{1}{2}\sum_{0}^{ne_B}\int^{l_e}\Bigg\{ & \frac{EA}{8}\left(2\mathbf{N}_{,x}\mathbf{u}^e + (\mathbf{H}_{,x}\mathbf{w}_b^e)^2 + 2(\mathbf{H}_{,x}\mathbf{w}_b^e)(\mathbf{H}_{,x}\mathbf{w}_s^e) + (\mathbf{H}_{,x}\mathbf{w}_s^e)^2\right)^2 \\ & + EI\left(\frac{(\mathbf{H}_{,xx}\mathbf{w}_b^e)^2}{2} + (\mathbf{H}_{,xx}\mathbf{w}_s^e)^2\left(\frac{1}{2} + \frac{3}{\pi^2} - \frac{24}{\pi^3}\right) + (\mathbf{H}_{,xx}\mathbf{w}_b^e)(\mathbf{H}_{,xx}\mathbf{w}_s^e)\left(1 - \frac{24}{\pi^3}\right)\right) \\ & + GA\frac{(\mathbf{H}_{,x}\mathbf{w}_s^e)^2}{4} + GAl^2\left(\frac{(\mathbf{H}_{,xx}\mathbf{w}_b^e)^2}{2} + \frac{(\mathbf{H}_{,xx}\mathbf{w}_s^e)^2}{2}\left(\frac{9}{16} - \frac{1}{\pi}\right)\right)\Bigg\}\mathrm{d}x \end{aligned} \tag{20}$$

with ne_B being the number of elements.

The kinetic energy in equations 12 can now be rewritten as

$$\begin{aligned} T_b = \sum_{0}^{ne_B}\int^{l_e}\Bigg\{ & \rho A\left[\frac{(\mathbf{N}\dot{\mathbf{u}}^e)^2}{2} + \frac{(\mathbf{H}\dot{\mathbf{w}}_b^e)^2}{2} + \frac{(\mathbf{H}\dot{\mathbf{w}}_b^e)^2}{2} + (\mathbf{H}\dot{\mathbf{w}}_b^e)(\mathbf{H}\dot{\mathbf{w}}_s^e)\right] \\ & + \rho I\left[\frac{(\mathbf{H}_{,x}\dot{\mathbf{w}}_b^e)^2}{2} + (\mathbf{H}_{,x}\dot{\mathbf{w}}_s^e)\left(\frac{1}{2} + \frac{3}{\pi^2} - \frac{24}{\pi^3}\right) + (\mathbf{H}_{,x}\dot{\mathbf{w}}_b^e)(\mathbf{H}_{,x}\dot{\mathbf{w}}_s^e)\left(1 - \frac{24}{\pi^3}\right)\right]\Bigg\}\mathrm{d}x \end{aligned} \tag{21}$$

The work of the electric force in (14) and the energy W_P in equation 15 can also be written in the form

$$W_F = \sum_{0}^{ne_B}\int^{l_e} q(x,t)(\mathbf{H}\mathbf{w}_b^e + \mathbf{H}\mathbf{w}_s^e)\mathrm{d}x \tag{22}$$

$$W_P = \sum\frac{1}{2}\int^{l_e} P\left((\mathbf{H}_{,x}\mathbf{w}_b^e)^2 + (\mathbf{H}_{,x}\mathbf{w}_s^e)^2 + 2(\mathbf{H}_{,x}\mathbf{w}_b^e)(\mathbf{H}_{,x}\mathbf{w}_s^e)\right)\mathrm{d}x \tag{23}$$

The element stiffness matrix derived from the strain energy of the beam can be written in sub-matrices as

$$\underset{(10\times10)}{\mathbf{k}_e} = \begin{bmatrix} \mathbf{k}_{aa} & \mathbf{k}_{ab} & \mathbf{k}_{as} \\ \mathbf{k}_{ab}^T & \mathbf{k}_{bb} & \mathbf{k}_{bs} \\ \mathbf{k}_{as}^T & \mathbf{k}_{bs}^T & \mathbf{k}_{ss} \end{bmatrix}, \tag{24}$$

The sub-matrices in the above equation are calculated by differentiating twice the beam strain energy in equation 20 as follows

$$\begin{aligned} & \underset{(2\times2)}{\mathbf{k}_{aa}} = \frac{\partial^2 U_b^e}{\partial(\mathbf{u}^e)^2},\ \underset{(4\times4)}{\mathbf{k}_{bb}} = \frac{\partial^2 U_b^e}{\partial(\mathbf{w}_b^e)^2},\ \underset{(4\times4)}{\mathbf{k}_{ss}} = \frac{\partial^2 U_b^e}{\partial(\mathbf{w}_s^e)^2}, \\ & \underset{(2\times4)}{\mathbf{k}_{ab}} = \frac{\partial^2 U_b^e}{\partial\mathbf{u}^e\partial\mathbf{w}_b^e},\ \underset{(2\times4)}{\mathbf{k}_{as}} = \frac{\partial^2 U_b^e}{\partial\mathbf{u}^e\partial\mathbf{w}_s^e},\ \underset{(4\times4)}{\mathbf{k}_{bs}} = \frac{\partial^2 U_b^e}{\partial\mathbf{w}_b^e\partial\mathbf{w}_s^e}, \end{aligned} \tag{25}$$

The element stiffness matrix stemming from the axial force P is of the form

$$\underset{(10\times10)}{\mathbf{k}_e^P}=\begin{bmatrix}\mathbf{0} & \mathbf{0} & \mathbf{0}\\ \mathbf{0} & \mathbf{k}_{bb}^P & \mathbf{k}_{bs}^P\\ \mathbf{0} & \left(\mathbf{k}_{bs}^P\right)^T & \mathbf{k}_{ss}^P\end{bmatrix},\ \underset{(4\times4)}{\mathbf{k}_{bb}^P}=\frac{\partial^2 W_P^e}{\partial(\mathbf{w}_b^e)^2},\ \underset{(4\times4)}{\mathbf{k}_{bs}^P}=\frac{\partial^2 W_P^e}{\partial(\mathbf{w}_b^e)\partial(\mathbf{w}_s^e)},\ \underset{(4\times4)}{\mathbf{k}_{ss}^P}=\frac{\partial^2 W_P^e}{\partial(\mathbf{w}_s^e)^2} \tag{26}$$

The element mass matrix can be also rewritten in sub- matrices as

$$\underset{(10\times10)}{\mathbf{m}_e}=\begin{bmatrix}\mathbf{m}_{aa} & \mathbf{m}_{ab} & \mathbf{m}_{as}\\ \mathbf{m}_{ab}^T & \mathbf{m}_{bb} & \mathbf{m}_{bs}\\ \mathbf{m}_{as}^T & \mathbf{m}_{bs}^T & \mathbf{m}_{ss}\end{bmatrix} \tag{27}$$

where

$$\begin{aligned}&\underset{(2\times2)}{\mathbf{m}_{aa}}=\frac{\partial^2 T_b^e}{\partial(\mathbf{u}^e)^2},\ \underset{(4\times4)}{\mathbf{m}_{bb}}=\frac{\partial^2 T_b^e}{\partial(\mathbf{w}_b^e)^2},\ \underset{(4\times4)}{\mathbf{m}_{ss}}=\frac{\partial^2 T_b^e}{\partial(\mathbf{w}_s^e)^2},\\ &\underset{(2\times4)}{\mathbf{m}_{ab}}=\frac{\partial^2 T_b^e}{\partial\mathbf{u}^e\partial\mathbf{w}_b^e},\ \underset{(2\times4)}{\mathbf{m}_{as}}=\frac{\partial^2 T_b^e}{\partial\mathbf{u}^e\partial\mathbf{w}_s^e},\ \underset{(4\times4)}{\mathbf{m}_{bs}}=\frac{\partial^2 T_b^e}{\partial\mathbf{w}_b^e\partial\mathbf{w}_s^e},\end{aligned} \tag{28}$$

Finally, the element vector of the nodal forces is

$$\underset{(10\times1)}{\mathbf{f}_e}=\left\{\mathbf{0}\quad \mathbf{f}_e^b\quad \mathbf{f}_e^s\right\}^T,\ \underset{(4\times1)}{\mathbf{f}_e^b}=\underset{(4\times1)}{\mathbf{f}_e^s}=\mathbf{H}^T q(x,t) \tag{29}$$

It should be noted that the electrostatic force $q(x,t)$ in the above equation, as defined by equation 13, is dependent on the current displacement $u_3(x,t)$. Thus, together with the large deflection, the dependence of the force on the displacement $u_3(x,t)$ is also a nonlinear source of this problem.

4. NUMERICAL PROCEDURE

To compute the frequencies of the microbeam in MEMS, the following two steps to be performed.

+ 1st step: the Newton-Raphson method is used to solve the following nonlinear equilibrium equation for the static displacements of the beams

$$\sum^{ne_B}\left(\left[\mathbf{k}_e(\mathbf{d}_e)+\mathbf{k}_e^P\right]\mathbf{d}_e-\mathbf{f}_e(\mathbf{d}_e)\right)=0 \tag{30}$$

+ 2nd step: using the obtained displacements, the elements stiffness matrices $\mathbf{k}_e(\mathbf{d}_e)$ and $\mathbf{k}_e^P$ in equations 24 and 26, respectively, are formed and assembled into the global stiffness matrix $[\mathbf{K}]$, and then the equation of motion for free vibration of the microbeam is constructed as

$$[\mathbf{M}]\ddot{\mathbf{D}}+[\mathbf{K}]\mathbf{D}=0 \tag{31}$$

where $\mathbf{M}$ is the global mass matrix of the microbeam.

By assuming a harmonic form for the displacements $\mathbf{D}$, equation 31 leads to the following eigenvalue equation

$$\left([\mathbf{K}]-\omega^2[\mathbf{M}]\right)\bar{\mathbf{D}}=0 \tag{32}$$

where ω and $\bar{\mathbf{D}}$ are the frequency and the eigenvector of the nodal displacements, respectively. The eigenvalue equation 32 is solved by the standard method [16] for the eigenfrequencies and eigenvectors.

5. NUMERICAL RESULTS

The effects of the loading and microscale parameters on frequencies of the microbeam are numerically investigated in this section. Otherwise mentioned, a clamped microbeam made from silicon with the following properties [17] is used in the investigation

$$E=169\text{GPa},\ \rho=2332\text{kg/m}^3,\ \nu=0.06 \tag{33}$$

For the convenience of discussion, the dimensionless fundamental frequency parameter (μ) and microscale parameter (η) are introduced as [16]

$$\mu=\omega_1\sqrt{\frac{\rho AL^4}{EI}},\quad \eta=\frac{l^2AG}{EI} \tag{34}$$

with ω_1 being the fundamental natural frequency.

The constraints for clamped boundaries are as follows $u_0 = w_b = w_s = w_{b,x} = w_{s,x} = 0$ at $x = 0, L$.

5.1. Verification

The derived formulation is firstly verified herewith. To this end, Figures 2 and 3 respectively show the curves of relation between the frequency parameter μ and the applied voltage of the microbeam without and with the axial force P for L = 210 μm, b = 100 μm, d = 1.18 μm, and η = 0, where for comparison the results of Ref. [17] are also given.

Table 1. Comparison of static pull-in voltages

Sources	L = 250 μm			L = 350 μm		
	P/A = -25	P/A = 0	P/A = 100	P/A = -25	P/A = 0	P/A = 100
Ref. [8]	33.04	39.13	58.84	13.27	20.36	36.99
Ref. [18]	33.70	39.50	56.90	13.80	20.30	35.40
Present	33.07	39.56	58.28	12.86	20.20	36.45
Error (%)	0.09 & 1.87	1.10 & 0.15	0.95 & 2.43	3.09 & 6.81	0.79 & 0.49	1.46 & 2.97

It can be seen from Figures 2 and 3 that the present results agree well with that of Ref. [17], irrespective of the axial force. One can see that the frequency parameter in the figures gradually decreases with increasing the voltage and it equals zero at the pull-in voltage. In Table 1, the static pull-in voltages of this paper are compared with the results of Ghazavi *et al.* [8], and Osterberg *et al.* [18] for a microbeam with b = 50 μm, h = 3 μm, d = 1 μm, and η = 0. Table 1 also shows that the pull-in voltages obtained herein agree well with that of the cited references, regardless of the beam length and the axial force. Noting that the Galerkin method with reduce-order model of beam is employed in [17], while Refs. [8] and [18] employed the finite difference method and the 3D MEMCAD model, respectively.

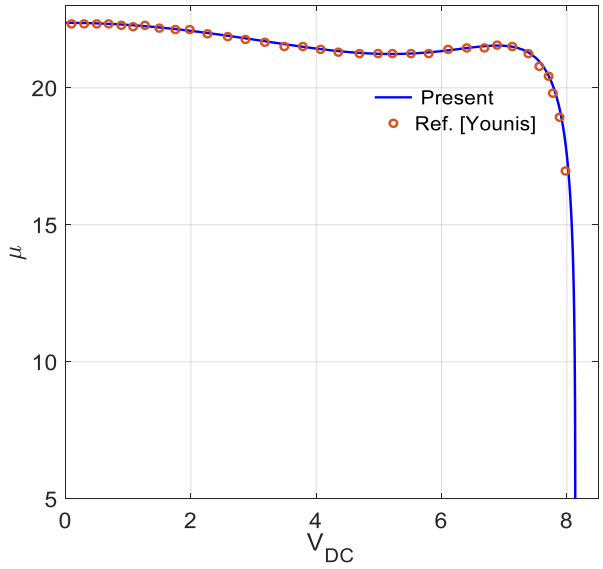

Figure 2. Relation between frequency parameter μ and applied voltage V_{DC} for $h = 0.6$ μm and without axial force (P=0)

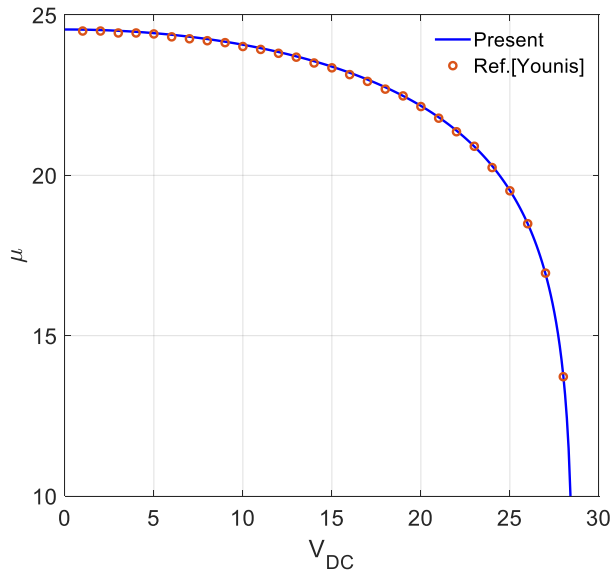

Figure 3. Relation between frequency parameter μ with applied voltage V_{DC} for $h = 1.5$ μm with an axial force P = -0.0009 N

5.2. Influence of the size effect

The influence of the microsize effect on the frequency parameters of the microbeam are shown in Table 2 and Figure 4. One can see from Table 2 and Figure 4 that both the parameter μ and the pull-in voltages are the compressive axial force amplitude for the beam associated with a large microscale parameter. The results in the table and the figure reveal that the microstructural effect has a significant influence on the frequency of the microbeam, and the frequency

parameter is considerably underestimated by ignoring the microsize effect. Furthermore, the pull-in voltage at which the fundamental frequency of the microbeam becomes zero is also increased with increasing the microscale parameter.

Table 2. Frequency parameters of MEMS microbeam with L=250 µm, b=100 µm, h=3µm, d=1 µm, P = -0.0008 N, and the different values of η and V_{DC}

V_{DC}(V)	0	5	10	15	20	25	30	35	40	45	50
η=0	21.99	21.94	21.78	21.49	21.03	20.33	19.16	16.83	-	-	-
η=0.1	23.10	23.05	22.90	22.63	22.20	21.56	20.55	18.75	13.08	-	-
η=0.2	24.16	24.11	23.97	23.71	23.31	22.72	21.82	20.32	17.01	-	-
η=0.3	25.17	25.13	24.99	24.74	24.36	23.81	23.00	21.71	19.26	-	-
η=0.4	26.15	26.10	25.97	25.73	25.38	24.86	24.11	22.96	20.98	15.41	-
η=0.5	27.08	27.04	26.91	26.69	26.35	25.86	25.16	24.12	22.44	18.82	-
η=0.6	27.99	27.95	27.83	27.61	27.28	26.82	26.16	25.21	23.74	20.97	-
η=0.7	28.87	28.83	28.71	28.50	28.19	27.74	27.13	26.25	24.93	22.65	15.94
η=0.8	29.72	29.68	29.57	29.36	29.06	28.64	28.05	27.23	26.03	24.08	19.74
η=0.9	30.55	30.51	30.40	30.20	29.91	29.50	28.95	28.17	27.07	25.35	22.03
η=1	31.36	31.32	31.21	31.02	30.74	30.35	29.81	29.08	28.05	26.51	23.78

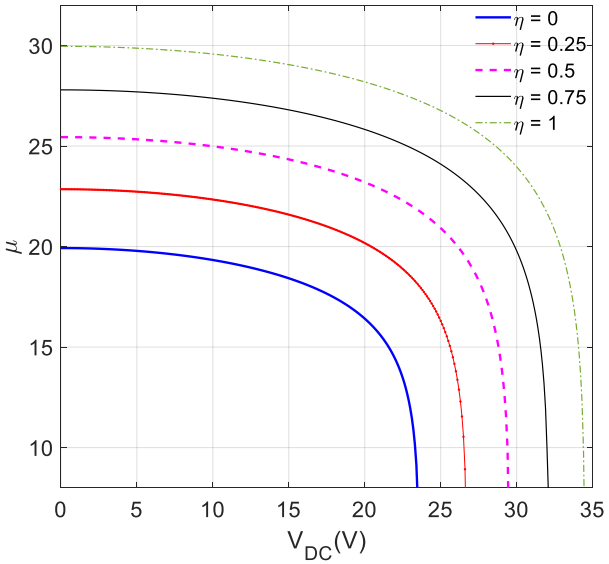

Figure 4. Variation of frequency parameter μ with applied voltage V_{DC} for L = 210 μm, b = 100 μm, h = 1.5 μm, d = 1.18 μm, P = -0.0009 N and various values of η.

5.3. Influence of the axial force

The influence of the axil force on the vibration behaviour of the microbeam in MEMS is illustrated in Table 3 and in Figure 5. As can be seen from the table and figure, the axial force has a significant influence on the frequency parameters as well as the pull-in voltages. The

increase of the amplitude of the compressive force (P < 0) results in an increase of the frequency. The effect of the tensile force (P > 0) is opposite, and the frequency decreases with increasing the tensile force. A similar influence of the axial force on the pull-in voltage can also be observed from Figure 5. The influence of the axial force on the frequency parameter can be explained by the fact that the flexural rigidity is reduced as the beam is subjected to a compressive axial force, and it is increased under a tensile axial force [19].

Table 3. Frequency parameters of microbeam MEMS with L = 250 μm, b = 100 μm, h = 3 μm, d = 1 μm, η = 0.25, and the variation of P and V_{DC}

V_{DC}(V)	0	5	10	15	20	25	30	35	40	45	50
P=-0.0030	23.75	23.70	23.56	23.29	22.88	22.27	21.34	19.74	15.84	-	-
P=-0.0024	24.01	23.96	23.81	23.55	23.15	22.55	21.64	20.11	16.60	-	-
P=-0.0018	24.26	24.21	24.07	23.81	23.41	22.82	21.93	20.46	17.27	-	-
P=-0.0012	24.51	24.46	24.32	24.06	23.67	23.09	22.23	20.81	17.86	-	-
P=-0.0006	24.75	24.71	24.56	24.31	23.93	23.36	22.51	21.14	18.41	-	-
P=0	24.99	24.95	24.81	24.56	24.18	23.62	22.79	21.47	18.91	-	-
P=0.0006	25.23	25.19	25.05	24.81	24.43	23.88	23.07	21.79	19.38	-	-
P=0.0012	25.47	25.43	25.29	25.05	24.68	24.14	23.34	22.10	19.82	5.71	-
P=0.0018	25.71	25.66	25.53	25.29	24.92	24.39	23.61	22.41	20.24	12.23	-
P=0.0024	25.94	25.90	25.76	25.53	25.16	24.64	23.88	22.70	20.64	14.24	-
P=0.0030	26.17	26.13	25.99	25.76	25.40	24.89	24.14	23.00	21.03	15.57	-

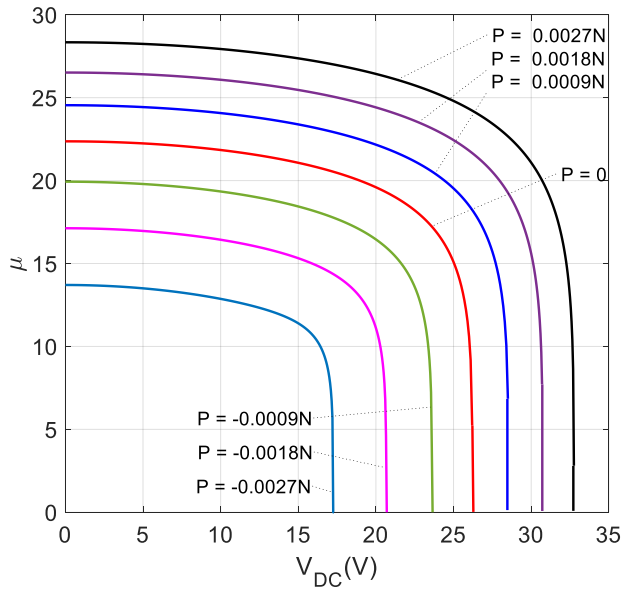

Figure 5. Frequency parameter μ versus applied voltage V_{DC} for L = 210 μm, b = 100 μm, h = 1.5 μm, d = 1.18 μm, η = 0 and various values of P

4. CONCLUSIONS

The free vibration of a microbeam with an axial force under electric actuation in MEMS has been investigated on the basis of the sinusoidal shear deformation theory and the MCST. Based on the von Kármán geometrically nonlinear assumption, a two-node beam element was formulated and employed to establish the discretized governing equations for the microbeam. Using the Newton-Raphson method, the deflections of the beams were firstly computed and then used to evaluate the tangent stiffness to construct the eigenvalue problem. The fundamental frequencies and the pull-in voltages were determined and the influence of the applied voltage, the axial force as well as the microsize effect on the vibration behaviour of the microbeam was examined in detail. The numerical results obtained in the present work showed that the axial force and the microsize parameter played an important role in the vibration frequencies and the static pull-in voltages of the beam. It has also been shown that the fundamental frequencies and the static pull-in voltage were considerably underestimated when the microstructural effect was ignored.

Acknowledgements. The work presented in this article was supported by the Vietnam Academy of Science and Technology (VAST), under Grant number CT0000.01/23-24.

CRediT authorship contribution statement. Cong Ich Le: Methodology, Software, Writing- Original draft preparation. Dinh Kien Nguyen: Supervision, Writing- Reviewing and Editing.

Declaration of competing interest. The authors declare that they have no known competing financial interests or personal relationships that could have appeared to influence the work reported in this paper.

REFERENCES

1. Choi B. and Lovell E. G. - Improved analysis of microbeams under mechanical and electrostatic loads, Journal of Micromechanics and Microengineering **7** (1) (1997) 24-29.
2. Abdel-Rahman E. M., Younis M. I. and Nayfeh A. H. - Characterization of the mechanical behavior of an electrically actuated microbeam, Journal of Micromechanics and Microengineering **12** (6) (2002) 759-766.
3. Younis M. I., Abdel-Rahman E. M., and Nayfeh A. - A reduced-order model for electrically actuated microbeam-based MEMS, Journal of Microelectromechanical systems **12** (5) (2003) 672-680.
4. Younis M. I. and Nayfeh A. H. - A study of the nonlinear response of a resonant microbeam to an electric actuation, Nonlinear Dynamics **31** (1) (2003) 91-117.
5. Abdel-Rahman E. M. and Nayfeh A. H. - Secondary resonances of electrically actuated resonant microsensors, Journal of Micromechanics and Microengineering **13** (3) (2003) 491-501.
6. Chaterjee S. and Pohit G. - A large deflection model for the pull-in analysis of electrostatically actuated microcantilever beams, Journal of sound and vibration. **322** (4-5), (2009) 969-986.
7. Ghazavi M. R., Rezazadeh G., and Azizi S. - Finite element analysis of static and dynamic pull-in instability of a fixed-fixed micro beam considering damping effects, Sensors & Transducers **103** (4), (2009) 132-143.

8. Rezazadeh G., Sadeghian H., Hosseinzadeh I. and Toloei A. - Investigation of pull-in phenomenon on extensible micro beam subjected to electrostatic pressure, Sensors & Transducers Journal. **79** (5) (2007) 1173-1179.
9. Kaneria A. J., Sharma D. S. and Trivedi R. R. - Static analysis of electrostatically actuated micro cantilever beam, Procedia Engineering **51** (2013) 776-780.
10. Farokhi H. and Ghayesh M. H. - Size-dependent behaviour of electrically actuated microcantilever-based MEMS, International Journal of Mechanics and Materials in Design **12** (3) (2016) 301-315.
11. Ghayesh M. H. and Farokhi H. - Nonlinear behaviour of electrically actuated microplate-based MEMS resonators, Mechanical Systems and Signal Processing. **109** (2018) 220-234.
12. Baghani M. - Analytical study on size-dependent static pull-in voltage of microcantilevers using the modified couple stress theory, International Journal of Engineering Science **54**, (2012), 99-105.
13. Ghayesh M. H., Farokhi H., and Amabili M. - Nonlinear behaviour of electrically actuated MEMS resonators, International Journal of Engineering Science **71** (2013) 137-155.
14. Yang F. A. C. M., Chong A. C. M., Lam D. C. C., and Tong P. - Couple stress based strain gradient theory for elasticity, International journal of solids and structures **39** (10) (2002) 2731-2743.
15. Thai H. T. and Vo T. P. - A new sinusoidal shear deformation theory for bending, buckling, and vibration of functionally graded plates, Applied Mathematical Modelling. **37** (5), (2013) 3269-3281.
16. Géradin M. and Rixen D. - Mechanical vibrations, Theory and Application to Structural Dynamics. John Wiley & Són, Chichester, 1997.
17. Younis M. I. - MEMS linear and nonlinear statics and dynamics (Vol. 20). Springer Science & Business Media, 2011.
18. Osterberg P. M. and Senturia S. D. - M-TEST: a test chip for MEMS material property measurement using electrostatically actuated test structures, Journal of Microelectromechanical systems **6** (2) (1997) 107-118.
19. Przemieniecki J. S. - Theory of Matrix Structural Analysis, McGraw-Hill Book Company, New York, 1985.